

MEASUREMENT OF GAMOW-TELLER AND SPIN DIPOLE STRENGTH IN THE $^{45}\text{Sc}(n, p)^{45}\text{Ca}$ REACTION AT 198 MeV

W.P. ALFORD¹, A. CELLER¹, B.A. BROWN², R. ABEGG³, K. FERGUSON,
R. HELMER³, K.P. JACKSON³, S. LONG⁴, K. RAYWOOD⁴ and S. YEN³

TRIUMF, 4004 Wesbrook Mall, Vancouver, B.C., Canada V6T 2A3

Received 15 November 1990

Abstract: The reaction $^{45}\text{Sc}(n, p)^{45}\text{Ca}$ has been studied at an energy of 198 MeV with energy resolution of about 1 MeV. Measurements were carried out at nominal angles 0° , 3° , 6° , 9° , 12° , 15° , 18° and spectra obtained up to ~ 40 MeV excitation energy in ^{45}Ca . Significant Gamow-Teller strength is observed at an excitation energy of about 7 MeV, somewhat higher than predicted by shell-model calculations. The strength observed is in agreement with calculations using $g_A/g_V \approx 1$. The spin-dipole giant resonance is seen with centroid at about 15 MeV excitation and total cross section of 25 mb/sr at an angle of 6° .

E

NUCLEAR REACTION $^{45}\text{Sc}(n, p)^{45}\text{Ca}$, $E = 198$ MeV; measured $\sigma(E_p, \theta)$. Deduced GT strength, spin-dipole σ . Shell model comparison.

1. Introduction

The distribution of Gamow-Teller (GT) strength for positron emission (or equivalently for electron capture) is of considerable interest for nuclei in the mass region $A \approx 56$, since electron capture on such nuclei is an important process in late stages of pre-supernova stellar evolution¹). It has been shown that the (n, p) reaction at intermediate energies provides a quantitative estimate of GT^+ strength²), and results have been reported for the $^{54}\text{Fe}(n, p)$ [ref. ³]) and $^{48}\text{Ti}(n, p)$ [ref. ⁴]) reactions. Similar information is needed for many more (fp) shell nuclei, however, including unstable species, and for excited states of the target nuclei which may be strongly populated at the high temperatures involved in supernova formation.

Since GT^+ strength distributions are unlikely to be measured for unstable targets or excited states, it is important to have reliable model calculations of these distributions. Calculations have been carried out for comparison with the measurements noted above, but they have provided only qualitative agreement with measured strength distributions. The problem stems from the fact that in general it is not yet

¹ Permanent address: University of Western Ontario, London, Ontario, Canada N6A 3K7.

² National Superconducting Cyclotron Laboratory and Dept. of Physics and Astronomy, Michigan State University, East Lansing, MI 48824, USA.

³ TRIUMF, 4004 Wesbrook Mall, Vancouver, B.C., Canada V6T 2A3.

⁴ University of Melbourne, Parkville, Victoria 3052, Australia.

feasible to carry out calculations in the full model space of the (fp) shell so that some truncation is required. As a result, a suitable nucleon–nucleon effective interaction is not as well determined as for the (sd) shell ⁵), where calculations are routinely carried out in the full model space.

The primary motivation for the present measurement comes from the fact that ^{45}Sc is the simplest (fp) shell nucleus with non-vanishing first-order GT^+ strength. For this particular case, it is possible to carry out calculations in the full (fp) shell model space; a comparison of such calculations with experiment will then be helpful in defining a suitable effective interaction for the (fp) shell. Given such an interaction, it will be interesting to study the effects of truncating the model space in calculations of GT strength for heavier (fp) shell nuclei.

2. Experimental

Measurements were carried out using the TRIUMF charge exchange facility in the (n, p) mode ⁶). The primary neutron beam was produced by the $^7\text{Li}(n, p)^7\text{Be}$ reaction at a nominal beam energy of 200 MeV. Four scandium targets of purity >99.99% (Johnson–Matthey Chemicals Ltd.) were mounted in a segmented target chamber ⁷), which also carried a polyethylene target in one position to provide a normalization of neutron flux via the $^1\text{H}(n, p)$ reaction. The scandium targets were 2.5 cm × 5 cm in size, with two targets 74 mg/cm² in thickness, and two of thickness 148 mg/cm². The spectrum of reaction protons up to an excitation energy of about 40 MeV in ^{45}Ca was measured at spectrometer angles of 0°, 3°, 6°, 9°, 12°, 15° and 18°. Because of the finite target size and finite spectrometer acceptance, reaction protons were recorded for a range of scattering angles of about ±2° about the nominal spectrometer setting. Data were recorded event by event, and the distribution of scattering angles was measured at each spectrometer angle. The mean scattering angle (c.m.) at each spectrometer angle was measured to be 1.8°, 3.4°, 6.0°, 9.1°, 12.1°, 15.1° and 18.2°.

Typical raw spectra at 0° and 6° are shown in fig. 1. The overall energy resolution is about 1 MeV. The peak near bin 12 in the 0° spectrum is a clear indication of GT strength. The peak at bin 6 arises from the $^1\text{H}(n, p)$ reaction on hydrogen in the wire chamber windows of the segmented target box ⁷). The intensity of this peak, plus other background due to counter gas and other materials in the chamber, was determined from background measurements with empty target frames in place of the scandium targets, and this background was then subtracted to yield the spectra due to scandium only, as shown in fig. 2. The subtraction removes the hydrogen peak at zero excitation, but otherwise has little effect on the spectrum. It should be noted that any hydrogen absorbed on the surface of the scandium targets would give a signal that would not be removed by this subtraction. Since the ground state Q -value for the $^{45}\text{Sc}(n, p)^{45}\text{Ca}$ reaction is 0.53 MeV, any signal due to residual hydrogen would be superimposed on that due to reaction protons leading to states

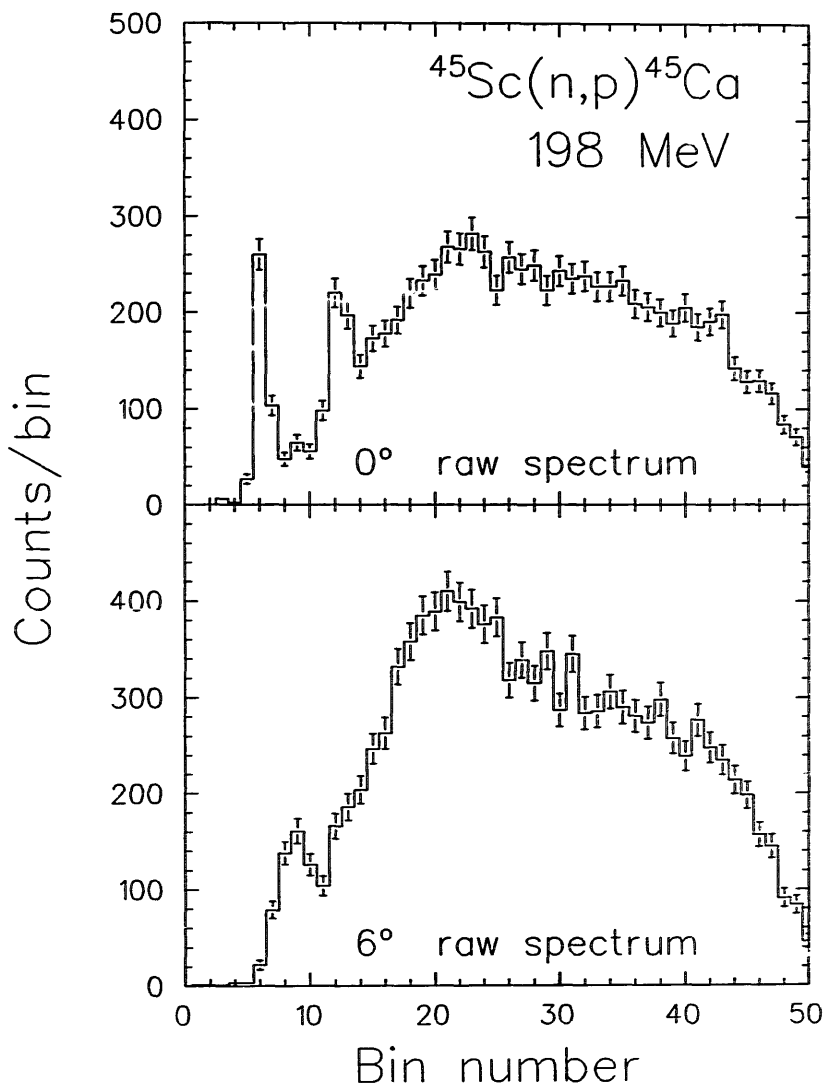


Fig. 1. Raw spectra for the $^{45}\text{Ca}(n,p)^{45}\text{Ca}$ reaction at spectrometer settings of 0° and 6° at 198 MeV. The peak at channel 6 in the 0° spectrum arises from the $^1\text{H}(n,p)$ reaction on hydrogen from Mylar in the wire chamber windows. The spectrum extends over a range of about 40 MeV of excitation in ^{45}Ca .

up to about 2 MeV in ^{45}Ca . Thus the data in this energy region provide only an upper limit to the cross section of interest.

Two further corrections to these spectra are required. The first arises from variations in spectrometer acceptance across the focal plane. These were determined by measuring the relative intensity of the proton peak from the $^1\text{H}(n,p)$ reaction as a function of position as the magnetic field of the spectrometer was varied. The second correction is required because of the low-energy continuum in the neutron spectrum from the $^7\text{Li}(p,n)^7\text{Be}$ reaction. This reaction yields a peak from the transitions to the ground and 0.43 MeV state of ^7Be , plus a continuum arising from transitions to unbound states which has an intensity of about 1% per MeV relative to the (g.s. + 0.43 MeV) peak. The effect of the continuum is readily deconvoluted from the data if it is assumed that the reaction cross section at a given excitation

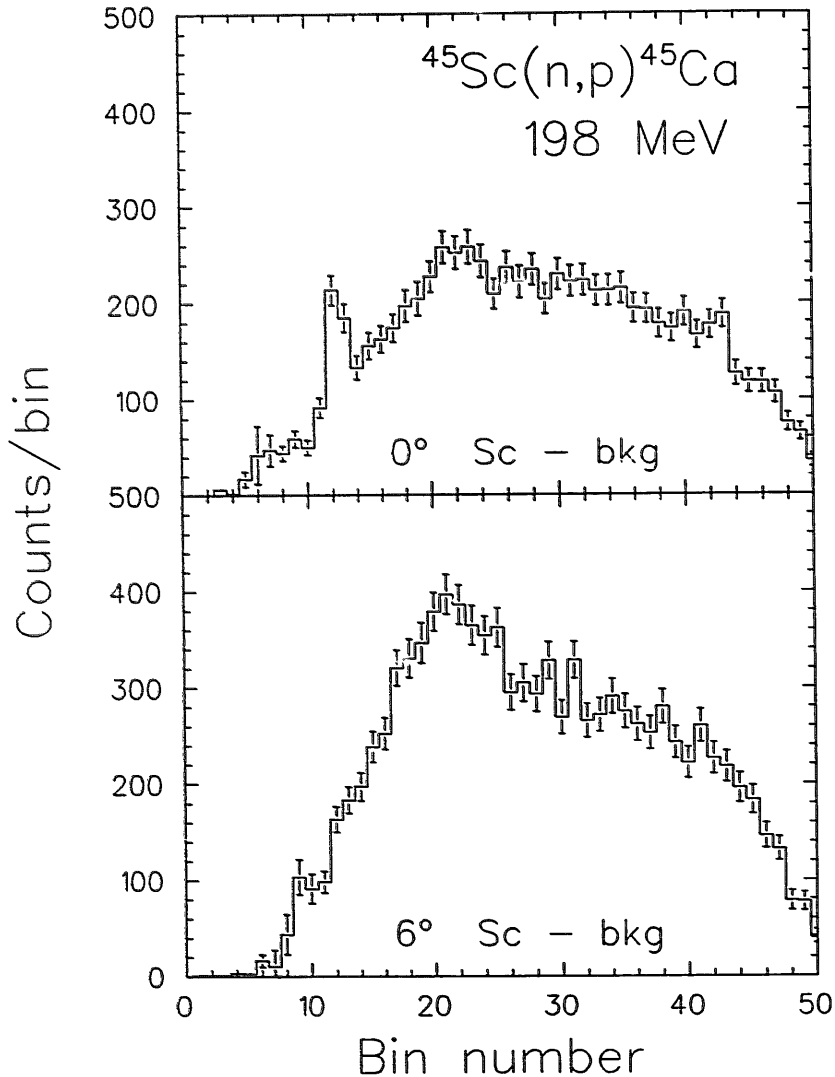


Fig. 2. Spectra of fig. 1 after background subtraction. Except for the hydrogen peak the background does not make a significant contribution to the cross section.

energy is independent of neutron energy. Final spectra with all corrections are shown in fig. 3.

As noted earlier, absolute cross sections were determined using a polyethylene foil in the target stack to monitor the neutron flux on the scandium targets. The $^1\text{H}(n,p)$ cross section was calculated to be 53.6 mb/sr at 1.8°_{lab} using the program SAID⁸⁾. A more detailed discussion of data analysis using this system is given in ref. ³⁾.

3. DWIA analysis

The zero degree spectrum in fig. 3 shows a clear peak at about 7 MeV excitation, indicating the presence of GT^+ strength. That peak is superimposed on a strong

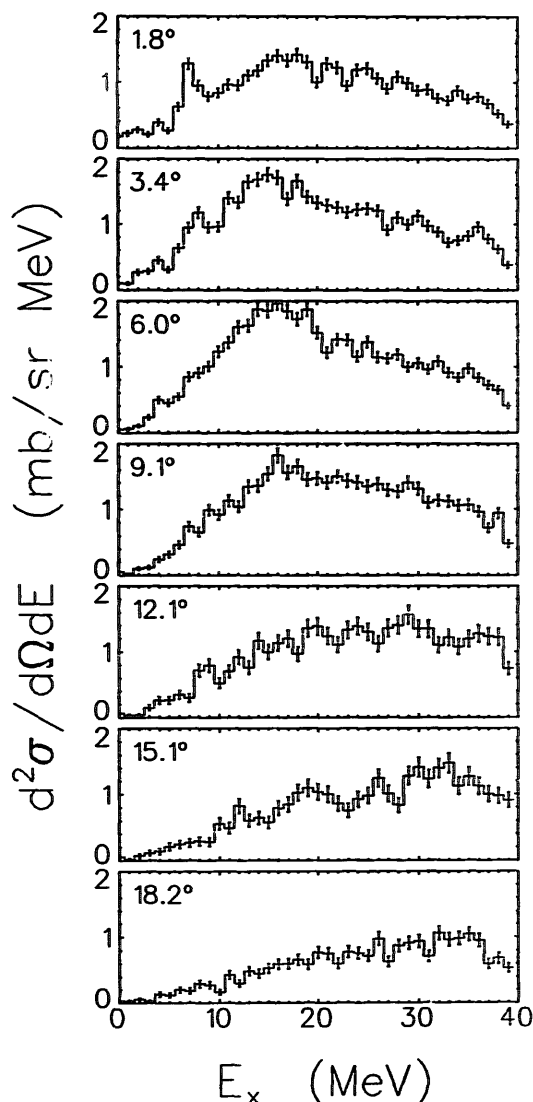


Fig. 3. Proton spectra from the $^{45}\text{Sc}(n, p)^{45}\text{Ca}$ reaction after correction for momentum dependence of spectrometer acceptance, and deconvolution of the contribution due to the continuum in the neutron source spectrum. The data have been rebinned into energy bins of 1 MeV width. The angle shown is the mean scattering angle over the MRS acceptance, transformed to the c.m. frame.

continuum however, which shows a maximum cross section at about 15 MeV excitation in the six-degree spectrum, suggesting the presence of the isovector spin dipole giant resonance. In order to obtain quantitative estimates of GT^+ and spin-dipole strength, and to separate these from other contributions to the spectra a multipole decomposition⁹⁾ was carried out by fitting measured spectra to a sum of shapes obtained by DWIA calculations for the L and J transfers expected to be significant in the data. To carry out this analysis, data at each angle were summed in energy bins 1 MeV in width, and the angular distribution for each bin was then independently fitted to a weighted sum of DWIA angular distributions using a least-squares fitting procedure to determine the fitting coefficients. For the fitting, the DWIA calculations were first convoluted with the measured angular acceptance

of the spectrometer in order to provide theoretical angular distributions directly comparable with the data.

In order to select a reasonable set of DWIA angular distributions to be used for the fitting, it was necessary to investigate the dependence of the theoretical distributions on several parameters of the DWIA calculations. For all values of angular momentum transfer $\Delta J^\pi = 0^-, 1^+, 2^+, 3^+$, calculations were carried out for a number of particle-hole configurations expected to be important. Fermi transitions with $\Delta J^\pi = 0^+$ were not considered since such transitions are forbidden in first order for nuclei with $N > Z$. The calculations were not extended to larger values of ΔJ^π , since the measured angular distributions contained only seven data points, and it was felt that the number of shapes used in the fitting should be limited to no more than four.

For $\Delta J^\pi = 1^+, 2^+, 3^+$ calculations were carried out for $0\hbar\omega$ excitations, assuming the initial proton to be in the $f_{7/2}$ shell model state. Angular distributions for $\Delta J^\pi = 1^+$ and 2^+ were not very sensitive to the final state assumed for the neutron, and could be characterized as $\Delta L = 0$ and $\Delta L = 2$ transitions, respectively. For 3^+ transitions the angular distributions were more sensitive to the neutron state, presumably reflecting the effect of $\Delta L = 4$ contributions in this case. Optical-model potentials used in the calculations were derived from the Franey-Love effective interaction¹⁰⁾ using a folding model. In addition, calculations were carried out for several particle-hole combinations using two different empirical potentials derived from elastic scattering data^{11,12)}. The shapes of the calculated angular distributions showed very little dependence on the optical potential used in the calculation, although the magnitudes varied by as much as 50% for different choices. All calculations for the final analysis were carried out using the microscopic potentials derived from the Franey-Love interaction.

Similar calculations were carried out for $\Delta J^\pi = 0^-, 1^-, 2^-, 3^-$ assuming particle-hole transitions with $1\hbar\omega$ excitation. The specific excitations assumed were $(2s1d) \rightarrow (fp)$ and $f_{7/2} \rightarrow (g_{9/2}, 3s2d)$. For each of the $0^-, 1^-,$ and 3^- transitions the calculated angular distributions showed characteristic shapes which did not depend strongly on the assumed particle-hole configuration, while 2^- transitions showed large variability because of the interference between $\Delta L = 1$ and $\Delta L = 3$ contributions to the transition amplitude.

The angular distributions calculated for several different particle-hole configurations for $\Delta J^\pi = 1^-$ are shown in fig. 4. All are characterized by a peak cross section in the angular region of 6° to 7.5° with differences at smaller and larger angles where the cross section is relatively small. Comparable results were found for $\Delta J^\pi = 1^+, 2^+$ and 3^- for which the peak cross section occurs at $0^\circ, 11^\circ-12^\circ$ and $16^\circ-18^\circ$, respectively.

The initial multipole analysis was carried out with the assumption that the data could be fitted with a superposition of shapes for $\Delta J^\pi = 1^+, 1^-, 2^+$ and 3^- , corresponding to $\Delta L = 0, 1, 2, 3$. Specific particle-hole combinations used in the DWIA

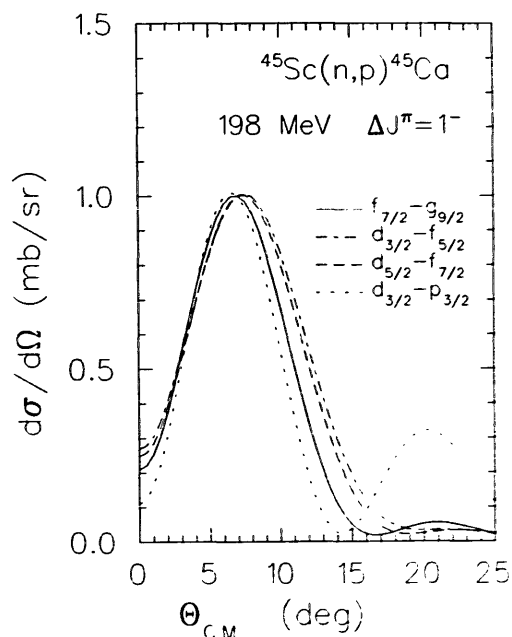


Fig. 4. Calculated angular distributions for $\Delta J^\pi = 1^-$ ($\Delta L = 1$) transitions for different particle-hole excitations. The DWIA results have been convoluted with the measured angular acceptance of the spectrometer and have all been normalized to the same peak cross section.

calculations were: 1^+ , 2^+ ($\pi^{-1}f_{7/2}$, $\nu f_{5/2}$); 1^- , 3^- ($\pi^{-1}d_{3/2}$, $\nu f_{5/2}$). The choice for the positive-parity transitions was influenced by the fact that both RPA calculations¹³⁾ and shell-model calculations reported here show that this is the most important component of the transition amplitude. There was no compelling reason for the choice for the negative-parity transitions, but the configuration chosen was judged to give a reasonable average representation of shapes resulting from a variety of different particle-hole combinations. As noted earlier, the calculated DWIA shapes were all convoluted with the measured angular acceptance of the MRS before comparison with the data.

The result of the multipole analysis for spectra at mean scattering angles of 1.8° , 6.0° and 12.1° is shown in fig. 5 where the contribution to the cross section for each J^π transfer is shown for each energy bin. An alternative representation of the result is shown in fig. 6. Here the magnitude of the fitting coefficient for each ΔJ^π is given as a function of excitation energy, along with the least-squares estimate of the uncertainty in each coefficient. Thus the data from fig. 6 provide an indication of the significance of the cross-section contributions shown in fig. 5.

From fig. 6 it is seen that the GT strength is concentrated near 7 MeV excitation, with an indication of strength between 10 and 20 MeV but with large systematic uncertainty. Above 20 MeV uncertainties in the analysis become so large that the significance of any $\Delta J^\pi = 1^+$ contribution in this region is questionable. $\Delta J^\pi = 1^-$ strength is well identified up to 20 MeV, and defines a giant resonance with centroid at about 15 MeV and width of 15 MeV. No significant cross section for $\Delta J^\pi = 2^+$ is found below 20 MeV, with some indication of a poorly defined giant resonance

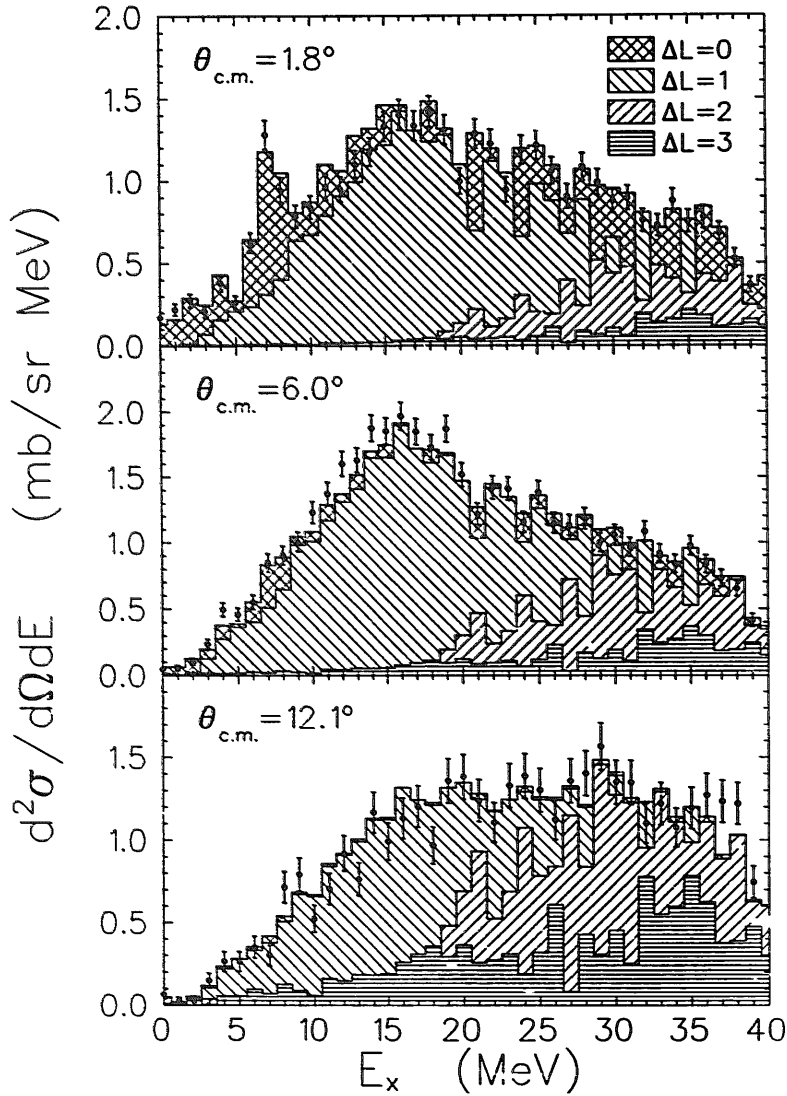


Fig. 5. Results of multipole analysis of the spectra at 1.8° , 6.0° and 12.1° . The DWIA calculations assumed particle-hole excitations $0\hbar\omega$, $(\pi^{-1}f_{7/2}, \nu f_{5/2})$ for $\Delta J^\pi = 1^+, 2^+$ ($\Delta L = 0, 2$) and $1\hbar\omega$, $(\pi^{-1}d_{3/2}, \nu f_{5/2})$ for $\Delta J^\pi = 1^-, 3^-$ ($\Delta L = 1, 3$).

between 20 and 30 MeV. Finally, there is a clear contribution for transitions with $\Delta J^\pi = 3^-$ which increases roughly linearly with excitation energy over the whole energy range of the data.

It should be noted that the multipole analysis is of questionable validity at high excitation in any case, since it is expected that $2\hbar\omega$ excitations for even-parity transitions and $3\hbar\omega$ for odd should begin to become important in this region. Some effort to include such excitations in the analysis was made, but with inconclusive results. A very large number of particle-hole configurations become possible, and DWIA shapes for a given ΔJ^π may depend strongly on the configuration assumed. At the same time, the experimental angular distributions show little structure in

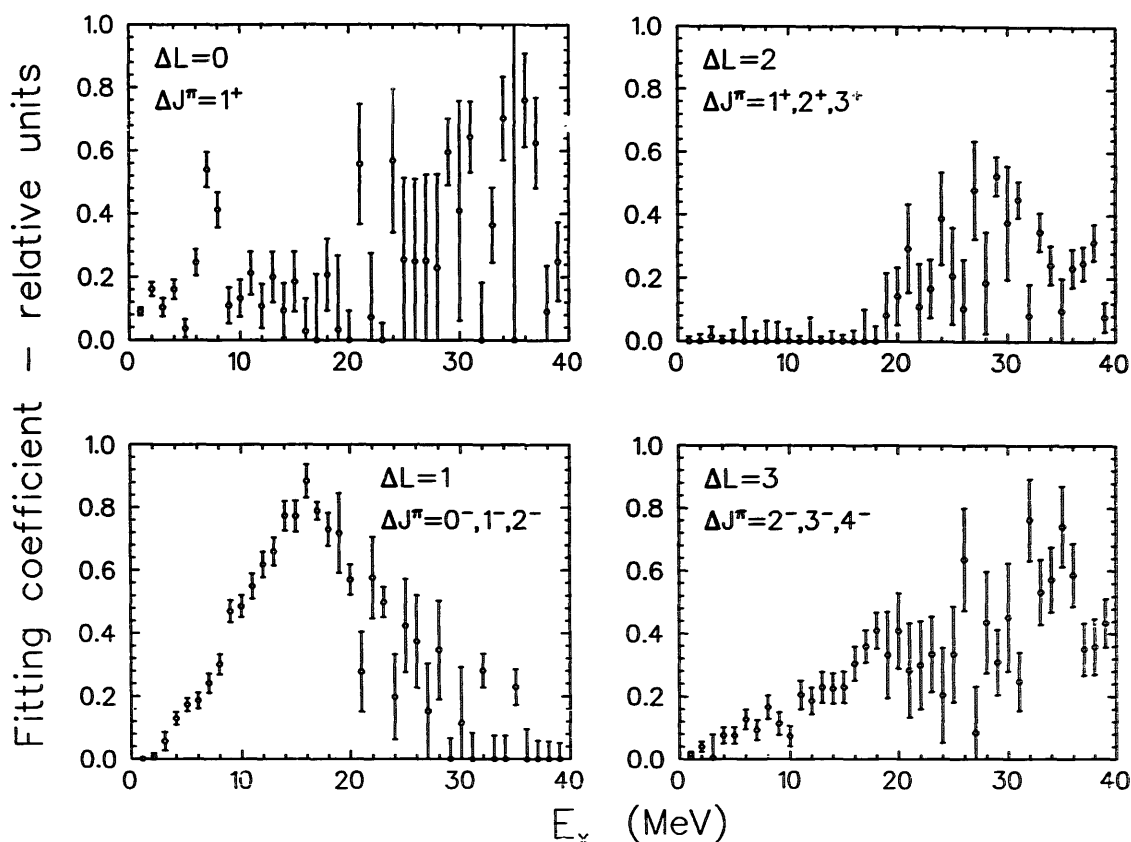


Fig. 6. Multipole fitting coefficients from the analysis shown in fig. 5. The bars on the points are an estimate of the uncertainty in the coefficient determined by the least-squares fitting program.

contrast to the data at lower excitation, where well-defined multipole contributions are identified. A realistic comparison with the data in this region would require DWIA calculations based on transition amplitudes generated by large-scale structure calculations such as those^{14,15}) which assume excitations over several oscillator shells. In the following discussion, only results for $E_x \leq 20$ MeV will be considered further.

An aspect of the analysis which is brought out in fig. 5 is that the fit to the measured angular distributions is relatively poor over the energy range from 11 to 16 MeV excitation. At 1.8° , the fitted cross section is consistently greater than the data in this range, while at 3.4° (not shown) and 6.0° it is consistently less. Several attempts were made to obtain a better fit using other combinations of particle-hole excitations for the DWIA calculations but no improvement was obtained.

DWIA calculations for $\Delta J^\pi = 0^-$ show a characteristic shape with a peak cross section in the range 4° to 5° , so that an analysis including a 0^- contribution might be expected to improve the fit. Consequently a multipole analysis was carried out assuming contributions from $\Delta J^\pi = 0^-, 1^+, 1^-, 3^-$. The DWIA calculation used a particle-hole configuration ($\pi^{-1}d_{5/2}, \nu f_{5/2}$) for 0^- . The component for $\Delta J^\pi = 2^+$ was not included since the first analysis showed that it did not contribute below 20 MeV and was of questionable significance at higher excitation.

The result of this second analysis for the fit to the data at 1.8° and 6.0° is shown in fig. 7, where it is seen that the fit is unchanged, except in the region between 11 and 16 MeV excitation where a significantly better fit is obtained. The fitting coefficients for this analysis are shown in fig. 8, and their significance is discussed in the following sections.

4. Discussion

4.1. GAMOW-TELLER STRENGTH

The cross section for $\Delta J^\pi = 1^+$ transitions which defines the GT strength is clearly concentrated in a peak near 7 MeV excitation. There is a small amount of strength at low excitation, although the apparent cross section below 2 MeV excitation might include some contribution from hydrogen in the targets, as noted earlier. In the first analysis shown in figs. 5 and 6 there was some indication of GT strength above 10 MeV excitation, but the significance of this is questionable. As shown in fig. 5, the fit to the angular distribution at 0° is relatively poor between 11 and 16 MeV excitation. Furthermore, fig. 6 shows that the uncertainty in GT strength estimated in this region is generally about the same magnitude as the fitted strength itself. The

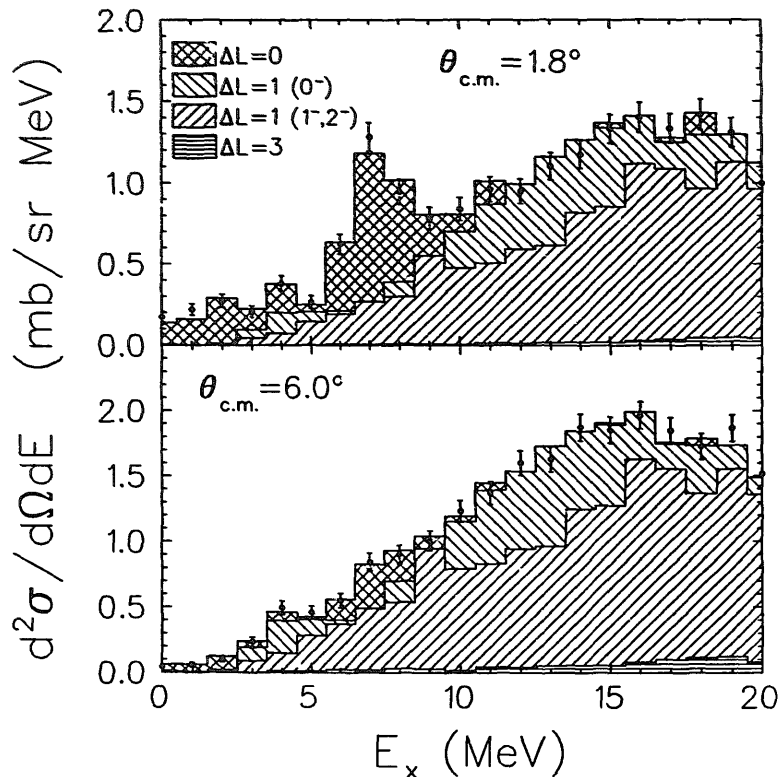


Fig. 7. Results of the multipole analysis of the spectra at 1.8° and 6.0° using DWIA shapes for $\Delta J^\pi = 0^-, 1^+, 1^-, 3^-$. The particle-hole excitations for $1^+, 1^-$ and 3^- were the same as for fig. 5. For 0^- it was $1\hbar\omega$, $(\pi^{-1}d_{5/2}, \nu 1^1_{5/2})$.

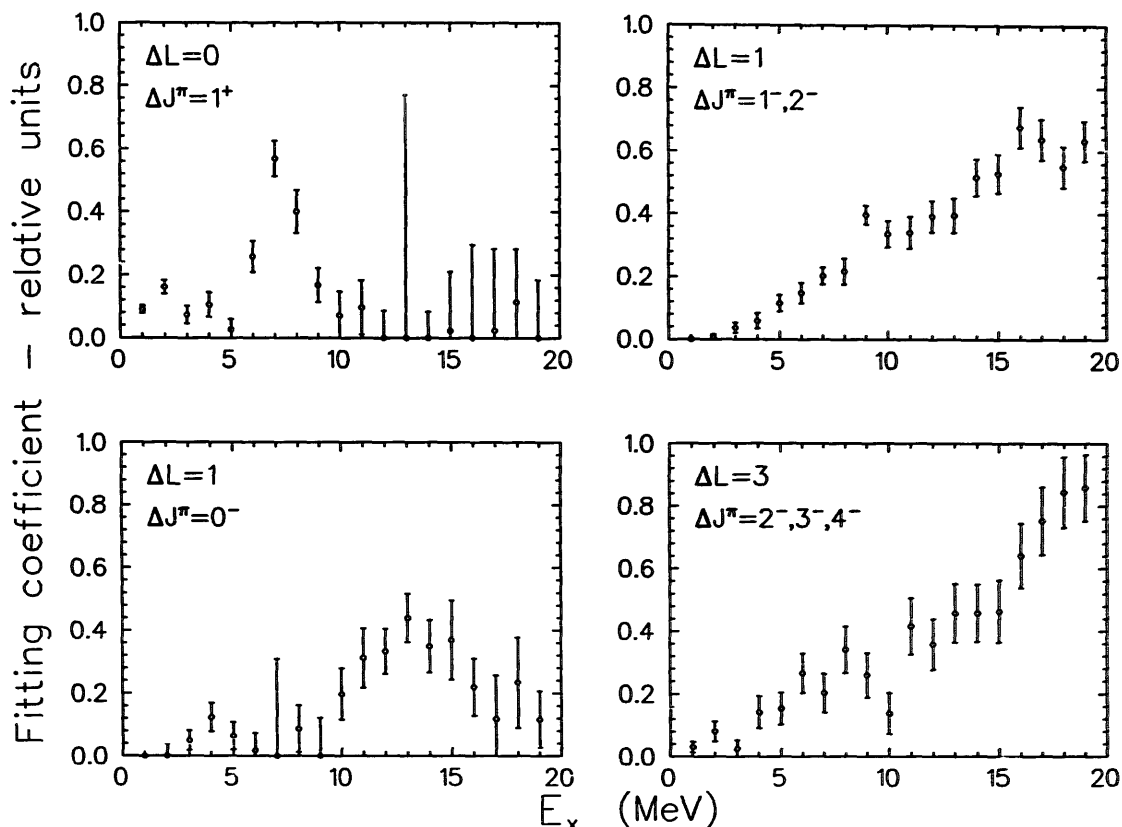


Fig. 8. Multipole fitting coefficients from the analysis shown in fig. 7.

second analysis, which includes $\Delta J^\pi = 0^-$ contributions, does not identify significant GT strength above 11 MeV. The uncertainty in measured strength is estimated to be about 15%, arising from statistical uncertainties in the data plus a contribution of about 10% from the fitting procedure in the multipole analysis.

The GT strength corresponding to the measured cross sections was obtained using the relation $\hat{\sigma} = \sigma(q = \omega = 0) / B_{\text{GT}} = 6.07$ mb/sr. This value was determined by fitting experimental values of $\hat{\sigma}$ to an expression of the form $\hat{\sigma}(A, E) = C_1(1 + C_2/E_p + C_3/E_p^2)(1 + C_4A^{1/3} + C_5A^{2/3})$ [ref. ¹⁶]. This is consistent with the value $\hat{\sigma} = 5.3$ mb/sr resulting from a comparable analysis in ref. ¹⁷). Values of $\sigma(q = \omega = 0)$ corresponding to the experimental data were obtained by using the DWIA calculations to determine the ratio $\sigma(q = \omega = 0) / \sigma(\theta = 1.8^\circ, \omega \neq 0)$. The definition of GT strength used here implies a value $B_{\text{GT}} = 3$ units for the decay of the free neutron.

A calculation of GT^+ strength in $^{45}\text{Sc}(n, p)^{45}\text{Ca}$ has been carried out using the full (fp) model space with an effective interaction derived by fitting energy levels in this mass region ^{18,19}). In this calculation, almost 90% of the strength is concentrated in two transitions to states with $J^\pi = \frac{5}{2}^-$ at energies of 5.29 MeV (84%) and 5.55 MeV (6%). The total predicted strength is 0.72 units, extending up to 13 MeV excitation.

A comparison between measured and calculated GT strength distributions is shown in fig. 9. The measured strength which results from the multipole analysis assuming a $\Delta J^\pi = 0^-$ component is concentrated in the energy range between 6 and 9 MeV, with a total strength of 0.46 units in this region. If this peak is compared with the peak predicted by the model calculations the results suggest a quenching of GT strength by a factor of 0.73, in agreement with usual estimates of quenching. However, additional strength amounting to 0.24 units is distributed more or less uniformly over the rest of the energy range up to 11 MeV, to give a total measured strength of 0.70 units with centroid at 7.6 MeV. This is very nearly equal to the total predicted strength, implying no quenching of the total strength, a result which has not been previously reported.

4.2. SPIN-DIPOLE STRENGTH

From the results of the multipole decomposition using DWIA shapes for $\Delta J^\pi = 1^+, 1^-, 2^+, 3^-$ as shown in fig. 6, the 1^- contribution is clearly defined up to an excitation energy of 20 MeV, with an indication of significant additional strength extending up to about 30 MeV. It should be noted that in this analysis the 1^- contribution is assumed to provide an estimate of contribution from all $\Delta L = 1$ spin-dipole components, i.e. $\Delta J^\pi = 0^-, 1^-$ and 2^- . This overall strength distribution appears as a giant resonance with a centroid energy of 13.6 MeV for transitions below 20 MeV

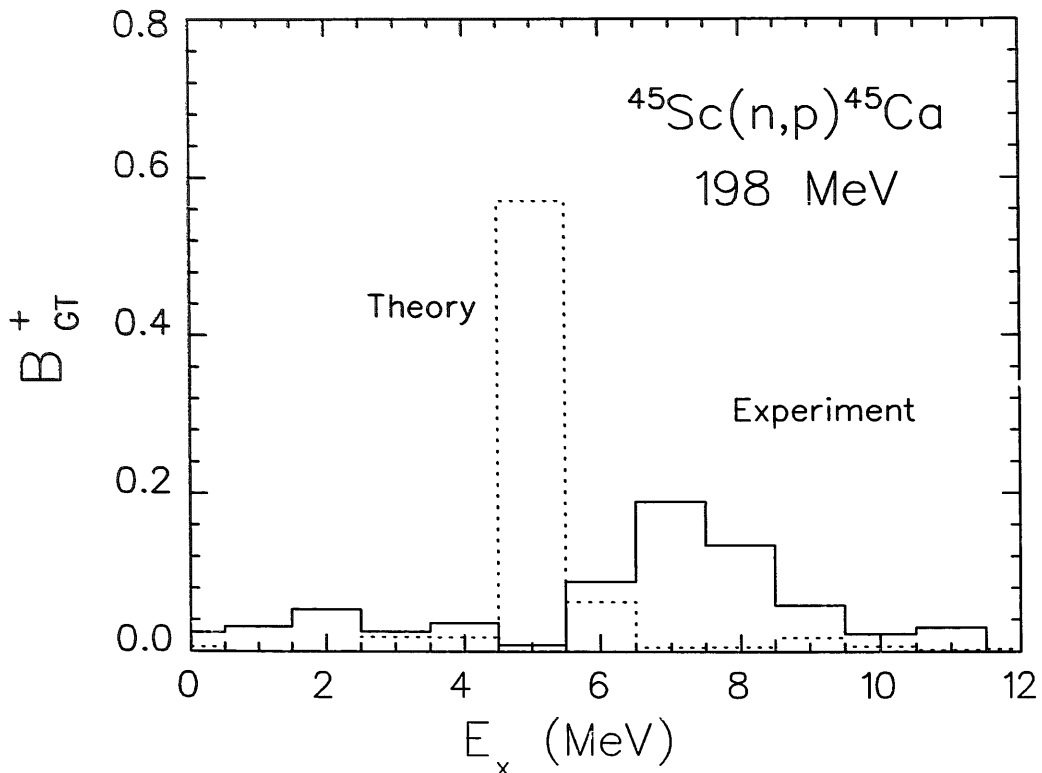


Fig. 9. Comparison of measured and calculated results for the distribution of Gamow-Teller strength for $^{45}\text{Sc}(n, p)^{45}\text{Ca}$.

or 16.5 MeV if the less certain strength up to 30 MeV is included. The energy-integrated cross section at 6° is 18.7 mb/sr up to 20 MeV and 24.8 mb/sr up to 30 MeV. The uncertainty in the total cross section up to 20 MeV is determined largely by the statistical uncertainty in the data, and is estimated to be about 10%. At higher excitation, the multipole analysis is subject to larger systematic uncertainties as noted earlier, and it is difficult to assign a total uncertainty to the cross-section estimate in that region. However, only about one-quarter of the total cross section lies above 20 MeV, so that the uncertainty in the overall sum is probably about 15 to 20%.

In the second analysis assuming contributions for $\Delta J^\pi = 1^+, 0^-, 1^-, 3^-$, the total cross section for $\Delta L = 1$ transitions is divided into two components. The component with $\Delta J^\pi = 0^-$ has an energy-integrated cross section at 6° of 5.6 mb/sr with a centroid energy of 12.1 MeV. The $\Delta J^\pi = 1^-$ component which is assumed to account for contributions with $\Delta L = 1$, $\Delta J^\pi = 1^-, 2^-$ has a cross section of 14.2 mb/sr with centroid energy of 13.6 MeV. If, in spite of systematic uncertainties, the analysis is extended to 30 MeV excitation, the 0^- cross section is almost unchanged, increasing from 5.6 mb/sr to 6.0 mb/sr. The 1^- cross section increases by the same amount as in the first analysis, from 14.2 mb/sr to 20.1 mb/sr with centroid energy of 17.2 MeV. The total cross section for $\Delta L = 1$ transitions at 6° is then 26.1 mb/sr, in good agreement with the earlier estimate of 24.8 mb/sr.

Estimates of the distribution of spin-dipole strength in medium-mass nuclei have been made by Bertsch, Cha and Toki²⁰⁾ using a Tamm-Dancoff approximation and by Auerbach and Klein¹³⁾ using a random-phase approximation. Both calculations conclude that the strength of 0^- and 1^- excitations should be fairly well localized in excitation, while the 2^- strength should be more widely distributed. They also conclude that the centroid of the 0^- strength should be located a few MeV above that of the sum of the 1^- plus 2^- strength. This conclusion is not very sensitive to details of the structure calculation and mainly reflects the influence of the spin-orbit part of the effective interaction. This is in disagreement with the results of the present analysis which finds the centroid of the 0^- strength lying well below that for the other $\Delta L = 1$ ($\Delta J^\pi = 1^-$ and 2^-) transitions.

In support of the experimental result, we note that the 0^- contribution to the multipole analysis was not included arbitrarily, but was introduced in order to account for the shape of the measured angular distributions in a well-defined, restricted region of excitation. The resulting analysis indicated the presence of 0^- strength in this region, as part of a fixed total strength for $L = 1$ transitions. Conclusions regarding strength for 1^+ transitions were not affected in the region of excitation below 12 MeV, where our estimate of GT strength is clearly significant and reliable. The present result probably represents the best that can be done in trying to separate different J transfers for a given ΔL , based on cross sections alone. Further progress in this direction will most likely require measurements of spin observables, as proposed for the (\vec{d} , ^2He) reaction for instance^{21,22)}.

4.3. TRANSITIONS WITH $L \geq 2$

The present measurements do not identify significant $L = 2$ strength at excitation energies below 20 MeV. There is an indication of some strength at higher excitation, but it is poorly determined, with very large uncertainties in its magnitude. This result suggests that if $\Delta L = 2$ transitions are present they are the result of $2\hbar\omega$ excitations generated¹³⁾ by an operator of the form $\sum_i r_i^2 (Y_2 \otimes \sigma_i)_\tau^J$, while $0\hbar\omega$ excitations are not important.

There is a clear indication of strength with $L = 3$ (actually $L \geq 3$) throughout the whole spectrum. The strength below 20 MeV is presumably the result of $1\hbar\omega$ excitations, analogous to the spin-dipole. Above 20 MeV it may be expected that $3\hbar\omega$ excitations will also contribute to the cross section. For this reason, no further analysis has been attempted, even though the multipole fitting coefficients indicate the presence of significant high-spin strength at high excitation.

5. Conclusions

A multipole analysis of the spectra reported here has provided a quantitative measurement of the distribution of GT^+ strength in ^{45}Ca . Although the result was obtained with a particular choice of particle-hole configurations in the DWIA calculations, the resulting distribution was found to be almost unchanged for other plausible choices. The results have been compared with predictions of a shell-model calculation using the full (fp) model space. The observed strength distribution is peaked at an excitation energy of 7 MeV, and is spread over several MeV, in contrast to the calculation which places about 90% of the predicted strength in two $\frac{5}{2}^-$ states between 5 and 5.5 MeV. Measured strength in the peak near 7 MeV is quenched by a factor of 0.73 relative to the calculated peak. The total strength over the energy range to 11 MeV is very nearly equal to the total calculated strength.

The initial multipole analysis provided clear evidence of a spin dipole giant resonance with a centroid near 15 MeV excitation and width of about 15 MeV. This analysis also showed some disagreement with experiment in the energy region between 10 and 15 MeV excitation, suggesting that transitions with $\Delta J^\pi = 0^-$ could be important in this region. A second analysis then indicated that the spin dipole cross section could be reliably separated into two components, one with $\Delta J^\pi = 0^-$ and one with $\Delta J^\pi = 1^-$ representing the remaining $\Delta L = 1$ strength. The sum of the cross sections for the two components was very nearly equal to that for 1^- transitions in the first analysis, and the measurement of GT^+ strength was unchanged. The centroid of the 0^- strength was found to lie about 3 MeV below that of the 1^- strength, in disagreement with results of RPA calculations.

The analysis showed no significant cross section with $\Delta L = 2$ below 20 MeV excitation. While there was some indication of such strength at higher excitation, it was not felt that the analysis was reliable in that region. Finally, the cross section

for transitions with $\Delta L \geq 3$ increases more or less linearly with energy, but no attempt was made to model this behaviour.

We wish to thank Dr. P. Green for his assistance with programming for the data acquisition system, P. Machule, R. Churchman and W. Felske also for extensive assistance with technical aspects of the apparatus. This work was supported by grants from the Natural Sciences and Engineering Research Council and the National Research Council of Canada. Part of this work was supported by the U.S. National Science Foundation grant number PHY87-14432.

References

- 1) J. Cooperstein and J. Wambach, Nucl. Phys. **A420** (1984) 591;
G.M. Fuller, W.A. Fowler and M.J. Newman, Astrophys. J. **293** (1985) 1;
M.B. Aufderheide, Nucl. Phys. **A526** (1991) 161
- 2) K.P. Jackson, A. Celler, W.P. Alford, K. Raywood, R. Abegg, R.E. Azuma, C.K. Campbell, S. El-Kateb, D. Frekers, P.W. Green, O. Häusser, R.L. Helmer, R.S. Henderson, K.H. Hicks, R. Jeppesen, P. Lewis, C.A. Miller, A. Moalem, M.A. Moinester, R.B. Schubank, G.G. Shute, B.M. Spicer, M.C. Vetterli, A.I. Yavin and S. Yen, Phys. Lett. **B201** (1988) 25
- 3) M.C. Vetterli, O. Häusser, R. Abegg, W.P. Alford, A. Celler, D. Frekers, R. Helmer, R. Henderson, K.H. Hicks, K.P. Jackson, R.G. Jeppesen, C.A. Miller, K. Raywood and S. Yen, Phys. Rev. **C40** (1989) 559
- 4) W.P. Alford, R. Helmer, R. Abegg, A. Celler, D. Frekers, P. Green, O. Häusser, R. Henderson, K. Hicks, K.P. Jackson, R. Jeppesen, C.A. Miller, A. Trudel, M. Vetterli, S. Yen, R. Pourang, J. Watson, B.A. Brown and J. Engel, Nucl. Phys. **A514** (1990) 49
- 5) B.H. Wildenthal, M.S. Curtin and B.A. Brown, Phys. Rev. **C28** (1983) 1343
- 6) R. Helmer, Can. J. Phys. **65** (1987) 588
- 7) R.S. Henderson, W.P. Alford, D. Frekers, O. Häusser, R.L. Helmer, K.H. Hicks, K.P. Jackson, C.A. Miller, M.C. Vetterli and S. Yen, Nucl. Inst. Meth. **A257** (1987) 97
- 8) R.A. Arndt and L.S. Roper, computer program SAID, unpublished
- 9) M.A. Moinester, Can. J. Phys. **65** (1987) 660
- 10) M.A. Franey and W.G. Love, Phys. Rev. **C31** (1985) 488
- 11) P. Schwandt, H.O. Meyer, W.W. Jacobs, A.D. Bacher, S.E. Vigdor, M.D. Kaitchuk and T.R. Donoghue, Phys. Rev. **C26** (1982) 55
- 12) A. Nadasen, P. Schwandt, P.P. Singh, W.W. Jacobs, A.D. Bacher, P.T. Debevec, M.D. Kaitchuk and J.T. Meek, Phys. Rev. **C23** (1981) 1023
- 13) N. Auerbach and A. Klein, Phys. Rev. **C30** (1985) 1032
- 14) F. Osterfeld, D. Cha and J. Speth, Phys. Rev. **C31** (1985) 372
- 15) R.D. Smith and J. Wambach, Phys. Rev. **C36** (1987) 2704
- 16) O. Häusser *et al.*, to be published
- 17) T.N. Taddeucci, C.A. Goulding, T.A. Carey, R.C. Byrd, C.D. Goodman, C. Gaarde, J. Larsen, D. Horen, J. Rapaport and E. Sugarbaker, Nucl. Phys. **A469** (1987) 125
- 18) L. Zhao, B.A. Brown and W.A. Richter, Phys. Rev. **C42** (1990) 1120
- 19) W.A. Richter, M.G. Van der Merwe, R.E. Julies and B.A. Brown, Nucl. Phys. **A523** (1991) 325
- 20) G. Bertsch, D. Cha and H. Toki, Phys. Rev. **C24** (1981) 533
- 21) C. Wilkin and D.V. Bugg, Phys. Lett. **B154** (1985) 243
- 22) C. Ellegaard, C. Gaarde, J.S. Jørgensen, J.S. Larsen, B. Million, C. Goodman, A. Brockstedt, P. Ekström, M. Österlund, M. Bedjidian, D. Contardo, D. Bachelier, J.J. Bayard, T. Hennino, J.C. Jourdain, M. Roy-Stephan, P. Radvanyi and P. Zupranski, Phys. Lett. **B231** (1989) 365